

Positional Offsets Between SiO Masers in Evolved Stars and their Cross-Matched Counterparts

YLVA M. PIHLSTRÖM,^{1,*} LORÁNT O. SJOUWERMAN,² MARK J CLAUSSEN,² MARK R. MORRIS,³ R. MICHAEL RICH,³
HUIB JAN VAN LANGEVELDE,^{4,5} AND LUIS HENRY QUIROGA-NUÑEZ^{4,5}

¹*Dept. of Physics and Astronomy, University of New Mexico, 1919 Lomas Boulevard NE, Albuquerque, NM 87131, USA*

²*National Radio Astronomy Observatory, 1003 Lopezville Road, Socorro, NM 87801, USA*

³*Department of Physics and Astronomy, University of California, Los Angeles, CA 90095-1547, USA*

⁴*Joint Institute for VLBI ERIC, Postbus 2, 7990 AA Dwingeloo, The Netherlands*

⁵*Leiden University, Postbus 9513, 2300 RA Leiden, The Netherlands*

(Accepted October 8, 2018)

ABSTRACT

Observations of dust-enshrouded evolved stars selected from infrared catalogs requiring high positional accuracy, like infrared spectroscopy or long baseline radio interferometric observations, often require preparational observational steps determining a position with an accuracy much better than 1". Using phase-referencing observations with the Very Large Array at its highest resolution, we have compared the positions of SiO 43 GHz masers in evolved stars, assumed to originate in their infrared detected circumstellar shells, with the positions listed in the *MSX*, *WISE*, 2MASS, and *Gaia* catalogs. Starting from an *MSX* position it is, in general, simple to match 2MASS and *WISE* counterparts. However, in order to obtain a *Gaia* match to the *MSX* source it is required to use a 2-step approach due to the large number of nearby candidates and low initial positional accuracy of the *MSX* data. We show that the closest comparable position to the SiO maser in our limited sample *never* is the *MSX* position. When a plausible source with a characteristic signature of an evolved star with a circumstellar shell can be found in the area, the best indicator of the maser position is provided by the *Gaia* position, with the 2MASS position being second-best. Typical positional offsets from all catalogs to the SiO masers are reported.

Keywords: catalogs – infrared: stars – masers – radio lines:stars – stars:AGB – surveys

1. INTRODUCTION

The Bulge Asymmetries and Dynamical Evolution (BAaDE) project is surveying more than 28,000 color-selected red giant stars in the Galactic plane for SiO maser emission (L.O. Sjouwerman et al., in prep.). With an instantaneous detection rate well over 50%, a unique sample of dynamical tracers in the plane is being constructed. At the frequencies of the SiO maser (43 GHz and 86 GHz) visual extinction is not a hinder, and extremely accurate line-of-sight stellar velocities ($\lesssim 2$ km s⁻¹) are determined at the locations of the stars (Habing et al. 1996, and references therein). The num-

ber of sources will be large enough to trace complex kinematic structures and minority populations. The velocity structure of these tracers will be compared with the kinematic structures seen in molecular gas and other objects near the Galactic Center, and thereby highlight kinematically coherent stellar systems, complex orbit structure in the bar, or stellar streams resulting from recently infallen systems. Investigations of the bar and bulge dynamics have begun using a subset of this new kinematic information in the inner Galaxy region (Trapp et al. 2018).

The BAaDE survey also identifies sufficiently luminous SiO masers suitable for follow-up parallax and proper motion determination using very long baseline interferometry (VLBI). With VLBI, it may be possible to investigate in detail orbits of stars constituting the stellar bar. Spectroscopic infrared (IR) data of the targets will also be taken to investigate metallicity effects

Corresponding author: Ylva Pihlström
ylva@unm.edu

* Y.M. Pihlström is also an Adjunct Astronomer at the National Radio Astronomy Observatory

across the bar and bulge region. Such follow-up studies require positional accuracies of the order of $0''.1$ or less. As the general BAaDE observing strategy using the NSF’s Karl G. Jansky Very Large Array (VLA) in the C and D configurations with resolutions of $1\text{--}2''$ utilizes the masers themselves for phase corrections (L.O. Sjouwerman et al., in prep.), the known positional accuracy is not improved beyond that of the initial *Midcourse Space Experiment* (*MSX*) positions ($1\text{--}2''$; Egan et al. 2003). To improve the SiO maser target positions, proper VLA A-array phase-referencing observations could be performed instead, pushing the accuracy down below $0''.01$, e.g. as shown here. However, doing such observations is impractical for several reasons. First, there are very few suitable VLA 43 GHz calibrators in the plane, severely limiting the number of sources that could be observed in this fashion. Second, phase referencing is time consuming, and re-observing the detected sample in this mode would in principle mean tripling our original time request at the telescope. Alternatively, we investigate whether cross-matching the parent *MSX* positions with other general all-sky IR and optical catalogs, like the Two-Micron All Sky Survey (2MASS; Skrutskie et al. 2006), the Wide-field Infrared Survey Explorer (*WISE*; Wright et al. 2010), and the *Gaia* Data Release 2 (DR2; Gaia Collaboration et al. 2016, 2018) with typical claimed absolute positional accuracies $\lesssim 0''.1$, can be used to improve the positional information. If so, the intermediate phase-referencing observations with the VLA in extended configurations may not be required to obtain sufficiently accurate positions for follow-up studies.

We here report on a limited study using the VLA in a regular phase-referencing observing scheme to determine the positions of a set of masers to $<0''.01$ accuracy. The resulting positions of the masers are compared to matched *MSX*, *WISE*, 2MASS and *Gaia* positions, in order to obtain a limited empirical determination of the positional agreement between the IR/optical and radio data. While some other catalogs with claimed accurate astrometry exist, they were not included in our study due to their more limited sky coverage.

2. DATA COLLECTION

2.1. Source Selection

Phase-referenced observations at the VLA were used to achieve accurate positions of the SiO maser. The accuracy of the derived positions depends in part on the goodness of the calibrated phases, requiring a bright calibrator source with good positional accuracy, located near the target field. The VLA calibrator J1755–2232 is positioned in the inner Galactic plane and has a listed

brightness of 0.32 Jy/beam in the VLA calibrator manual along with an absolute positional accuracy quoted between $0''.002\text{--}0''.01$, and was therefore chosen to be the phase-referencing calibrator. Within a distance of $0''.6$ of J1755–2232, 33 previously BAaDE detected SiO maser stars were observed in this experiment. The initial field centers used for observing these targets were the *MSX* positions included in Table 1.

2.2. VLA Observations and Data Reduction

The sources were observed in June 2015¹ under project code 15A-497 with the VLA in the A-array configuration, yielding an angular resolution of about 50-100 milli-arcsecond (mas). The Doppler-shifted frequencies of both the $^{28}\text{SiO}(1\text{--}0)$ $v = 2$ and $v = 1$ lines were covered by our setup (600 km s^{-1} total velocity bandwidth). A phase-referencing cycle time of 50 seconds was used, with 20 seconds on the calibrator bracketing each target source, which in turn was observed for 30 seconds. Each target was observed twice, resulting in a typical 1.7 km s^{-1} (250 kHz) channel rms noise of 13 mJy/beam, agreeing with the estimated theoretical rms noise for observations at low elevations and 1 minute on-source integration.

The data were calibrated using the AIPS package, and a deconvolved map of each maser was constructed using the CLEAN algorithm with a robust weighting of zero. The resulting synthesized beam sizes were almost identical, $0''.128 \times 0''.045$ at a position angle of 30° . Of the 33 targets 26 were detected. Because SiO masers are variable throughout the stellar cycle with a period of a few hundred days, this is a likely reason for the seven non-detections. For the detections, a two-dimensional Gaussian fit was performed to determine the peak flux position of the emission, listed as the VLA positions in Table 1, determined from the channel with peak emission of the $v = 1$ or $v = 2$ lines. On average the signal-to-noise ratio (S/N) of the detection in one channel was 25, leading to $1\text{-}\sigma$ uncertainties in the reported SiO positions of about 1.0 mas in x and 2.8 mas in y using the relation $\Delta\theta_i = (0.54\theta_i)/(S/N)NR$, where θ_i is the full-width at half maximum of the synthesized beam in the i -direction (Reid et al. 1988). Given the beam position angle, the resulting errors in Right Ascension (R.A.) and declination (decl.) are approximately 0.8 and 2.4 mas. Spectra of these sources, along with the line properties, will be published as part of the main BAaDE project; see L.O. Sjouwerman et al. (in prep.).

2.3. MSX, WISE and 2MASS Data

¹ This date, 2015.5, coincides with the epoch of *Gaia* DR2.

Table 1. Source VLA and IR/optical catalog positions

VLA		MSX		WISE		2MASS		Gaia	
R.A. (h:m:s)	decl. ($^{\circ}$: $'$: $''$)	R.A. (m:s)	decl. ($'$: $''$)	R.A. (m:s)	decl. ($'$: $''$)	R.A. (m:s)	decl. ($'$: $''$)	R.A. (m:s)	decl. ($'$: $''$)
17:57:45.7491	-22:40:37.634	57:45.74	40:37.9	57:45.748	40:37.60	57:45.747	40:37.62	57:45.7487	40:37.635
17:56:35.1030	-22:38:16.087	56:35.09	38:16.1	56:35.118	38:15.92	56:35.110	38:15.91	56:35.1038	38:16.066
17:57:16.8026	-22:37:19.622	57:16.78	37:21.0	57:16.802	37:19.47	57:16.810	37:19.56	57:16.8023	37:19.631
17:57:37.7290	-22:37:07.215	57:37.73	37:08.0	57:37.738	37:07.15	57:37.730	37:07.27	57:37.7296	37:07.201
17:57:32.9523	-22:33:21.200	57:32.93	33:22.3	57:32.955	33:21.18	57:32.961	33:21.03	57:32.9523	33:21.200
17:57:32.1456	-22:30:19.551	57:32.09	30:20.5	57:32.139	30:19.49	57:32.147	30:19.58	57:32.1452	30:19.555
17:55:19.7673	-22:28:49.418	55:19.82	28:49.1	55:19.757	28:49.44	55:19.773	28:49.43	55:19.7672	28:49.415
17:53:17.0344	-22:26:02.737	53:17.06	26:02.4	53:17.034	26:02.61	53:17.040	26:02.70	53:17.0352	26:2.7303
17:57:33.5178	-22:24:26.355	57:33.50	24:28.1	57:33.543	24:26.07	57:33.522	24:26.19	57:33.5195	24:26.340
17:54:53.7339	-22:22:30.810	54:53.76	22:30.4	54:53.750	22:31.00	54:53.740	22:30.60	54:53.7356	22:30.809
17:53:29.5411	-22:21:46.851	53:29.59	21:47.2	53:29.538	21:46.82	53:29.542	21:46.77	53:29.5411	21:46.854
17:56:48.5306	-22:17:41.335	56:48.50	17:42.4	56:48.552	17:41.29	56:48.542	17:41.35	56:48.5303	17:41.347
17:57:16.5811	-22:15:20.805	57:16.56	15:21.6	57:16.594	15:20.90	57:16.590	15:20.69	-	-
17:56:22.7935	-22:13:48.308	56:22.78	13:50.2	56:22.794	13:47.76	56:22.792	13:48.15	56:22.7939	13:48.312
17:54:52.1393	-22:11:00.323	54:52.15	11:01.0	54:52.140	11:00.31	54:52.147	11:0.319	54:52.1394	11:0.3669
17:55:04.2674	-23:11:22.130	55:04.20	11:21.8	55:04.271	11:22.07	55:04.261 ^a	11:22.03	55:04.2651	11:22.159
17:54:10.0437	-23:06:36.299	54:10.06	06:35.6	54:10.039	06:36.13	54:10.047	06:36.25	54:10.0436	06:36.289
17:56:11.9651	-23:04:28.685	56:12.02	04:27.8	56:11.978	04:28.06	56:11.959	04:28.70	56:11.9648	04:28.683
17:54:16.2127	-23:02:35.897	54:16.20	02:35.2	54:16.216	02:35.80	54:16.212	02:35.98	54:16.2126	02:35.885
17:55:05.1692	-23:01:42.724	55:05.21	01:41.9	55:05.169	01:42.54	55:05.173 ^a	01:42.54	55:05.1679	01:42.730
17:54:16.7405	-23:01:36.955	54:16.75	01:36.5	54:16.748	01:36.93	54:16.742	01:36.98	54:16.7398	01:36.947
17:53:56.1170	-23:00:23.772	53:56.06	00:23.4	53:56.128	00:24.95	53:56.112	00:23.70	53:56.1170	00:23.763
17:53:30.2574	-22:55:30.018	53:30.22	55:29.3	53:30.252	55:29.85	53:30.253 ^a	55:29.76	53:30.2569	55:30.009
17:57:06.7550	-22:44:54.598	57:06.77	44:54.6	57:06.740	44:54.40	57:06.764	44:54.47	57:06.7552	44:54.596
17:55:32.0723	-22:05:07.412	55:32.06	05:08.5	55:32.060	05:07.62	55:32.068	05:07.43	55:32.0726	05:07.416
17:54:11.9268	-22:03:57.408	54:11.95	03:57.6	54:11.960	03:57.53	54:11.930	03:57.42	54:11.9274	03:57.407

^aTwo candidate matches were found within the $5''$ search radius. The selected cross-match is the reddest, brightest and also the closest candidate.

The BAaDE sources were originally selected from the *MSX* Point Source Catalog version 2.3 (Egan et al. 2003), based on their IR color in order to optimize for the detection of SiO masers (Sjouerman et al. 2009). The *MSX* mission was designed to collect IR photometry along the full Galactic plane, and in regions not covered by *IRAS*. For regions toward the Galactic center in particular, where *IRAS* was heavily confused due to the high source density, *MSX* significantly improved existing IR catalogs. *MSX* has a beam of $18''3$, with astronomically useful bands observed at 8.3, 12.1, 14.7 and $21.3 \mu\text{m}$ (bands *A*, *C*, *D*, and *E*, respectively). The *MSX* positional information is dominated by information from band *A* as it is the most sensitive band along with having the shortest wavelength. The *MSX* astrometric accuracy depends on the detection quality (Egan et al. 2003), and the sources selected for the BAaDE sample used quality

photometry flags $Q_X \geq 3$ (i.e., 3 and 4) where Q_X indicates the quality in band *X*, translating into a positional accuracy between $0''.80$ – $1''.7$.

Based on the *MSX* positions and their accuracy, for each *MSX* position with a maser detected, a search radius of $5''$ was used to search the NASA/IPAC Infrared Science Archive (IRSA) for cross-matches in the *WISE* and 2MASS surveys, with the results listed in Table 1.

The *WISE* survey scanned the sky at 3.6, 4.6, 12 and $22 \mu\text{m}$ (bands W1, W2, W3, and W4, respectively) with angular resolutions of $6''.1$, $6''.4$, $6''.5$ and $12''.0$. Initially, the *WISE* All-Sky catalog positions were referenced with respect to the 2MASS catalog, giving accuracies of $\approx 0''.15$, but the more recent All *WISE* catalog has since improved upon the accuracy to $< 0''.1$ by also implementing proper motion for reference objects. Within the search radius only single cross-matches were found,

with reported *WISE* positional accuracies of on average $0''.035$ and $0''.036$ in R.A. and decl.

The 2MASS project observed the full sky with a resolution of $2''$, using the 1.24 , 1.66 and $2.16\mu\text{m}$ (J , H , and K_s) bands (Skrutskie et al. 2006). Cross-matches to all of our SiO maser detected *MSX* sources were found in the 2MASS Point Source Catalog, with three fields showing two possible cross-matches within the search radius (marked in Table 1). Given the anticipation of our targets being dust-enshrouded evolved stars, most likely asymptotic giant branch (AGB) stars, the source which was reddest and brightest was selected, which in all three cases also corresponded to the closest match in position. The quoted accuracies for all 2MASS positions are $0''.06$ in both R.A. and decl.

2.4. Gaia Data

The *Gaia* mission is conducting a full sky survey at $0.7\mu\text{m}$ (G -band). Although the spectral energy distribution (SED) from dust-enshrouded stars has its peak in the (near-)IR, the specific selection for stars with thinner shell envelopes in the BAaDE survey (i.e., Miras instead of OH/IR stars) allows on occasion for optical emission being detected, for example, by *Gaia*. Whereas we do not anticipate many *Gaia* counterpart matches in the most obscured regions in the Galactic plane and for the thicker shell objects in the entire BAaDE sample, the sensitive *Gaia* data is expected to yield some counterpart matches that can be studied here along with the IR catalogs.

The *Gaia* DR2 provides high quality astrometric data (Gaia Collaboration et al. 2018; Lindegren et al. 2018), which was used to search for cross-matches to our SiO maser sample. The *Gaia* data, however, had to be treated differently than the IR data, as searching within 5 arcseconds of the *MSX* positions provides up to 8 matches for individual *MSX* sources. Given the uncertainty in the *MSX* positions, a smaller search radius could not be applied without the risk of missing the correct cross-match. To ensure the correct candidate was selected, color and brightness criteria were applied, similar to what was done for the 2MASS multiple candidates (Sect. 2.3). *Gaia* DR2 contains photometry for the full G band covering 0.33 - $1.05\mu\text{m}$, and for some sources also the photometry and associated color measured with the integrated G_{BP} and G_{RP} bands at 0.33 - $0.68\mu\text{m}$ and 0.63 - $1.05\mu\text{m}$, respectively (Evans et al. 2018). As the targeted objects typically are large-amplitude variable stars, another characteristic that could be used in ensuring a proper cross-match is a variability indication. Only one candidate counterpart with this information was found in the *Gaia* data for our sample, and thus

we ignored this characteristic further in our matching scheme². In addition, the positional offsets between the *Gaia*-selected candidates and the VLA SiO masers, as well as the offsets between the *Gaia* candidates and the previously cross-matched 2MASS positions were considered to aid in the *Gaia* cross-matching procedure:

- For the set of 26 masers, one source had no *Gaia* candidate cross-match at all, possibly due to optical extinction. Note that this region around the calibrator is at G006.63+1.38, a region for which not much extinction is expected, which may explain the large fraction of optical counterparts. The remaining 25 sources had a combined number of 78 candidate cross-matches in the *Gaia* DR2 catalog within a $5''$ radius of the *MSX* position. The *Gaia* G band magnitude was collected for all 78 candidates, as was the $G_{BP} - G_{RP}$ color, which existed for 47 candidates.
- A cross-match was determined to be the most likely match if the $G_{BP} - G_{RP}$ color (if existing) was the reddest amongst the candidates, and if the positional offset to the SiO maser was the smallest and $< 0''.5$. For 14 of the 25 sources with *Gaia* data, such cross-matches existed. It turns out that for all these 14 sources, also the *Gaia*-2MASS offset was consistently the smallest and $< 0''.5$.
- Subsequently, returning to the original 78 candidates and selecting on *Gaia*-2MASS offsets only, the same 14 candidates with *Gaia* colors were selected along with 11 additional cross-matches for those lacking color information³.

Figure 1 presents a color-magnitude diagram showing the distribution of the 47 candidate cross-matches within $5''$ (crosses) on top of a set of 5,758 randomly selected *Gaia* sources in the neighborhood of our targets, illustrating the spread of the colors of the candidates. We note that, assuming an $M_{\text{bol}} \approx -6$ for the brightest AGB stars, a *Gaia* magnitude fainter (larger) than 12 for this sample (Fig. 1) also indicates that our counterparts are more distant than 4 kpc. We therefore may ignore any *Gaia* parallax (i.e., $\pi < 0.25$ mas) and proper motion⁴ corrections here. The 14 circles denote

² For calculating a measure of variability other than using the *Gaia* DR2 variability flag, see e.g. Quiroga-Nuñez et al. (2018); Belokurov et al. (2017). This is beyond the scope of this paper.

³ This implies that a 2-step matching scheme, following the sequence *MSX*→2MASS→*Gaia*, is the best approach also when no accurate phase-referenced SiO maser positions are available as is the case for the majority of the BAaDE sample.

⁴ See first footnote.

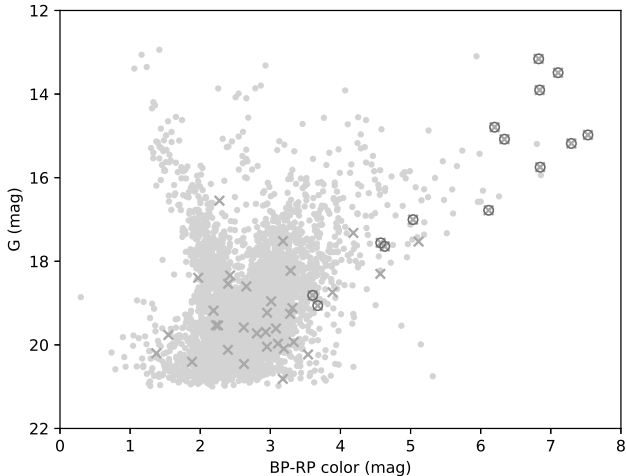


Figure 1. A *Gaia* color-magnitude diagram, with 5,758 randomly selected sources in the neighborhood of the calibrator and target SiO masers plotted as light gray dots. All the 47 *Gaia* candidate matches for which *Gaia* colors were available are marked by crosses, showing the spread in the diagram of all candidates. After applying an angular distance offset and a color criterion, the 14 circles denote the selected cross-matches. This illustrates that the applied selection methodology primarily chooses redder and brighter stars, consistent with our targets being mainly redder dust-enshrouded (AGB) stars.

the position in the diagram of the candidates with reddest color and offsets $<0''.5$ from the SiO masers. This demonstrates that the selected cross-matches belong to the overall redder and brighter population of stars, consistent with them being redder dust-enshrouded (AGB) stars. The linearly averaged reported accuracies for the *Gaia* positions of these faint sources were, on average, 0.99 mas (R.A.) and 0.64 mas (decl.).

3. RESULTS

The attainable accuracy of the derived maser positions depends on the size of the synthesized beam and the signal-to-noise ratio of the detection, but the absolute positional accuracy of the phase-referencing calibrator also has to be considered. The VLA calibrator manual classifies the position of J1755–2232 to be between $0''.002$ – $0''.01$ accurate. Conservatively assuming the larger value, an error of 10 mas would be dominating the error of the derived maser positions. By shifting the calibrator data during the calibration procedure, we instead used the position obtained from the Radio Fundamental Catalog (RFC⁵), providing sub-mas accuracies of 0.16 mas and 0.28 mas in R.A. and decl., respectively.

⁵ <http://astrogeo.org/rfc/>

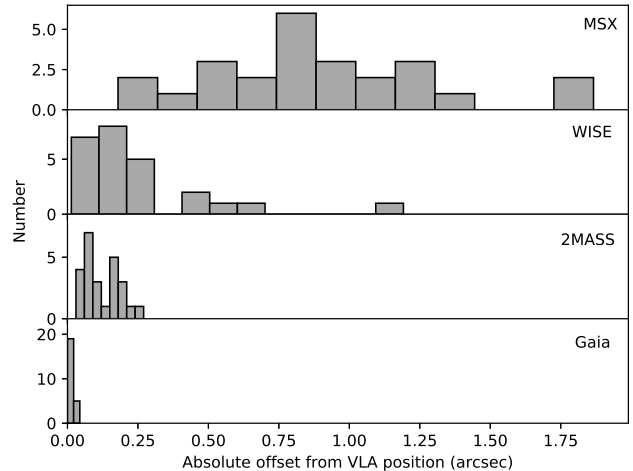


Figure 2. Measured absolute offsets in arcseconds between the VLA SiO maser positions and the *MSX*, 2MASS, *WISE* and *Gaia* positions. The closest positional match is provided by *Gaia* if available, and by 2MASS otherwise.

The position used was (J2000) R.A. $17^h55^m26.284535^s$, decl. $-22^\circ32'10.61573''$, which is 22 mas from the VLA catalog position. As a result, the positional errors of the calibrator combined with the VLA-derived errors are governed by the 0.8 and 2.4 mas VLA maser errors in R.A. and decl., respectively. This is much smaller than the typical quoted absolute values of $1''.7$, $0''.035$ and $0''.060$ errors, respectively, for the *MSX*, *WISE* and 2MASS catalogs, and of the same order as the error for the *Gaia* catalog; the *Gaia* positional accuracy is thus directly comparable to that of the derived VLA maser positions.

3.1. Total and systematic offsets

To determine how close the IR/optical catalog positions are to the VLA SiO maser position, offsets were calculated between the VLA and *MSX*, 2MASS, *WISE*, and *Gaia* matches respectively. Figure 2 plots the offset distribution, showing that the *MSX* positions can always be improved using any of the other catalogs considered here. Furthermore, positions are best matched using *Gaia* positions when available, next followed by 2MASS. This is further illustrated in the scatter plot of the positions as a function of R.A. and decl., where the *Gaia* and 2MASS positions are tightly clustered around the VLA maser positions (Fig. 3). The mean offsets between the SiO masers and *MSX*, *WISE*, 2MASS and *Gaia* catalogs are $0''.89$, $0''.26$, $0''.12$ and $0''.01$, respectively.

Along with Fig. 3, Fig. 4 separates the spread in the positional offsets into R.A., and decl. components, in order to consider any systematic offsets for any of the

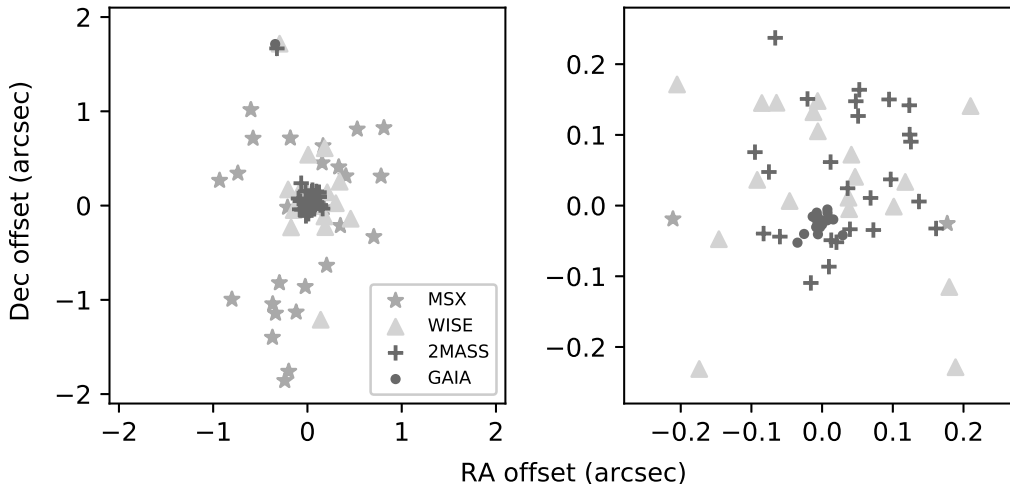


Figure 3. Diagram of measured offsets in arcseconds between the VLA SiO maser positions and the *MSX*, *WISE*, 2MASS and *Gaia* positions. The panel on the left hand side shows the full distribution (which is located well within the $5''$ search radius), while the right hand side is a zoom of the central region to emphasize the even closer match of the *Gaia* versus 2MASS positions.

surveys. There is a weak trend of the 2MASS data preferentially reporting a more northern declination than the SiO masers, and conversely, that the *MSX* data reports a more Southern declination.

4. DISCUSSION

The data confirm that *Gaia* positions are superior in pinpointing the stellar SiO maser emission if it can be matched. This is not surprising, given that the SiO masers arise close to the central star, at the inside of the larger circumstellar envelope (CSE) where dust and other molecules are residing. SiO masers are further known to be ubiquitous in AGB stars with thin CSEs, allowing for the central star to still be detectable in the optical. If a *Gaia* match is not obtainable, for example for more optically obscured or thicker shell objects, 2MASS will provide a very good option for improving the positional accuracy compared to any of the other IR catalogs. We here discuss reasons for why the *WISE* positions appear to be less accurate in tracing the masers (4.1) and how the detection rates in the BAaDE SiO maser survey are improved using 2MASS positions (4.2).

4.1. *WISE* versus 2MASS positions

It is clear that the 2MASS positions are more accurate than *WISE* in predicting the SiO maser positions, despite the better quoted positional accuracy of *WISE*. There are several possible causes for this; first, *WISE* data has an intrinsically worse resolution (wider point spread function). By inspecting the fields around the targets in the IRSA database, we noted that some of the 2MASS targets have multiple possible matches, which

likely are confused in the *WISE* data. Secondly, the turnover of the SED for these sources tend to occur around $1\text{-}2\ \mu\text{m}$, with the *WISE* bands at longer wavelengths being sensitive for emission from the CSE. Like for *Gaia*, the shorter 2MASS wavelengths are more likely to directly probe the central star, which will then better pinpoint the stellar position no matter how far the CSE extends or how asymmetric the CSE is. The SiO masers are known to occur within a couple to a few stellar radii (Diamond et al. 1994; Perrin et al. 2015), inside the main circumstellar shell and close to the dust condensation radius, beyond which the SiO becomes locked up in dust grains. The *WISE* data will be more dominated by the full extent of the CSE, and despite a quasi-spherical mass loss assumed during the AGB phase, the larger size overall will likely make it more difficult to exactly measure the position of the central star. We assume that this effect is worse for *MSX*, which operated at even longer wavelengths than *WISE*.

4.2. Improved detection rate in the BAaDE survey

As this program intended to improve initial positions from the *MSX* catalog and to assert what positions to use for VLBI, applying *Gaia* or 2MASS positions to our VLA survey should improve our maser detection rate. For the 28,000 star BAaDE survey, we rely on an assumed high detection rate initially and then utilize the detected masers to perform self-calibration, applying the resulting phase corrections to nearby targets lacking detections (L.O. Sjouwerman et al., in prep.). The self-calibration procedure prevents improved positional information to be derived, as is usually obtained in the more commonly applied phase-referencing

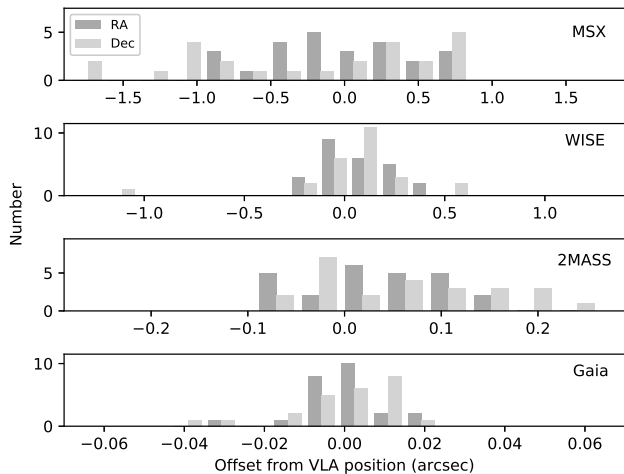


Figure 4. R.A., (dark gray) and decl. (light gray) offsets in arcseconds between the VLA SiO maser positions and the *MSX*, *WISE*, 2MASS and *Gaia* positions. Note the difference in scale in the offsets for the different catalogs.

scheme. This strategy has the clear advantage that it removes hundreds of calibration hours using the sparse high-frequency weather needed for our survey, and still provides velocities along with positions. However, in regions of the sky where the source density is lower our calibration scheme is less effective, and every detection is crucial for the calibration of neighboring targets. Especially for weaker masers, a positional error of $1 - 2''$ could result in the maser not being detected in our pipeline which considers emission to be at the phase center (read *MSX* position), thereby reducing the effectiveness of our calibration strategy. Exchanging the *MSX* positions with *Gaia* or 2MASS positions in the self-calibration scheme should improve our detection rate and thus the efficiency of the survey overall.

While approximately 30% of our BAaDE sample may be expected to be detected in the *Gaia* DR2 catalog (a full cross-match is currently under way), 96% have cross-matches in the 2MASS survey. Hence we focused on using the 2MASS cross-matches in the VLA campaign. While the *Gaia* positions would be preferable for VLBI 43 GHz observing, the BAaDE survey is performed in C- and D-configuration at the VLA. With a resulting synthesized beamwidth of $0''.5 - 1''.5$, 2MASS positions are sufficiently accurate and there should be little difference in the detection rate using *Gaia* instead of 2MASS positions. We consequently tested our VLA BAaDE pipeline on a random typical observing run by shifting the sources from the originally observed *MSX* positions to their corresponding 2MASS positions, and then re-running the pipeline. While the original data reduction reported 208 detections, using the 2MASS po-

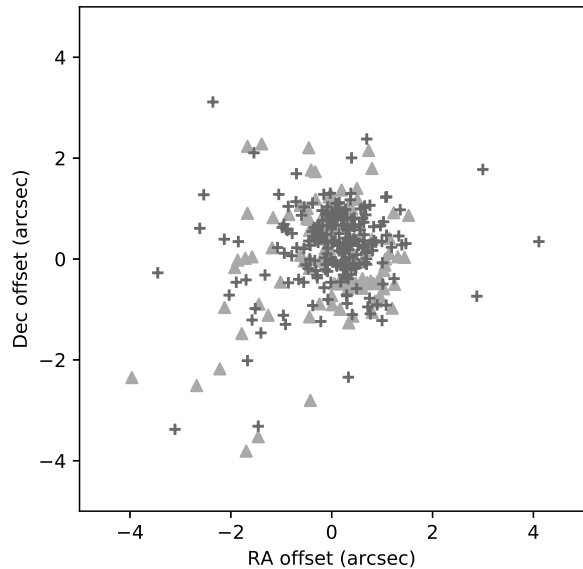


Figure 5. Distribution of the shifts (in arcseconds) applied to a set of sources in a BAaDE observing run, from *MSX* to 2MASS positions. Triangles denote sources that were detected using the *MSX* positions, while the plus-signs indicate the *additional detections* made by shifting targets to 2MASS positions. No initial detections were lost in the process.

sitions the number increased to 347, thus a 40% increase in the detection rate (see Fig. 5). All of the originally detected sources were detected with the 2MASS positions, thus the introduced shifts did not shift any sources outside the beam.

5. CONCLUSIONS

By comparing stellar SiO maser positions derived from VLA phase-referencing observations to those listed by the *MSX*, *WISE*, 2MASS and *Gaia* catalogs, we have found that it is always preferred to replace the *MSX* positions with positions from other catalogs and that *Gaia* positions most closely match those of the SiO masers (typically within $\sim 0''.01$). For follow-up work, or new work done by pre-selecting targets using IR colors, the results can be significantly improved by performing cross-matching to either the 2MASS or the *Gaia* (matched to the 2MASS counterpart) catalogs and using their positional information. The mean offsets between the SiO masers and *MSX*, *WISE*, 2MASS and *Gaia* catalogs are $0''.89$, $0''.26$, $0''.12$ and $0''.01$, respectively. The SiO maser emitting stars considered contain thin CSEs. For objects with thicker shells, and for other work in optically obscured regions, using 2MASS positions should be sufficient. For follow-up VLBI work, additional matching to *Gaia* positions is clearly pre-

ferred.

The BAaDE project is funded by National Science Foundation Grants 1517970 (UNM) /1518271 (UCLA).

The National Radio Astronomy Observatory is a facility of the National Science Foundation operated under cooperative agreement by Associated Universities, Inc.

This research made use of data products from the Midcourse Space Experiment. Processing of the data was funded by the Ballistic Missile Defense Organization with additional support from NASA Office of Space Science.

This research has also made use of the NASA/ IPAC Infrared Science Archive, which is operated by the Jet Propulsion Laboratory, California Institute of Technology, under contract with the National Aeronautics and Space Administration.

This publication makes use of data products from the Two Micron All Sky Survey, which is a joint project

of the University of Massachusetts and the Infrared Processing and Analysis Center/California Institute of Technology, funded by the National Aeronautics and Space Administration and the National Science Foundation.

This publication makes use of data products from the Wide-field Infrared Survey Explorer, which is a joint project of the University of California, Los Angeles, and the Jet Propulsion Laboratory/California Institute of Technology, funded by the National Aeronautics and Space Administration.

This work has made use of data from the European Space Agency (ESA) mission *Gaia* (<https://www.cosmos.esa.int/gaia>) processed by the *Gaia* Data Processing and Analysis Consortium (DPAC, <https://www.cosmos.esa.int/web/gaia/dpac/>) Funding for the DPAC has been provided by national institutions, in particular the institutions participating in the *Gaia* Multilateral Agreement.

Facilities: VLA, IRSA, WISE, MSX, 2MASS, Gaia

REFERENCES

- Belokurov, V., Erkal, D., Deason, A.J., Koposov, S.E., De Angeli, F., Evans, D.W., Fraternali, F., Mackey, D. 2017, *MNRAS*, 446, 4711
- Diamond, P.J., Kembell, A.J., Junor, W., et al. 1994, *ApJ*, 430, L61
- Egan, M.P., Price, S.D., Kraemer, K.E., et al. 2003, The Midcourse Space Experiment Point Source Catalog, Version 2.3, Air Force Research Laboratory Technical Report AFRL-VS-TR-2003-1589 (Springfield, VA: NTIS)
- Evans, D.W., Riello, M., De Angeli, F. et al., 2018, *A&A*, 614, A4
- Prusti, T., de Bruijne, J.H.J., Brown, A., et al., 2016, *A&A*, 595, A1
- Brown, A.G.A., Vallenari, A., et al., 2018, *A&A*, 616, A1
- Habing, H. 1996, *ARA&A*, 7, 97
- Lindgren, L., Hernández, J., Bombrun, A., et al., 2018, *A&A*, 616, A2
- Perrin, G., Cotton, W.D., Millan-Gabet, R., et al. 2015, *A&A*, 576 70
- Quiroga-Nuñez, L.H., van Langevelde, H.J., Pihlström, Y.M., et al., 2018, in: Recio-Blanca, A., de Laverny, P., Brown, A.G.A., & Prusti, T., (eds.) , *Astrometry and Astrophysics in the Gaia sky*, Proc. IAU Symposium No. 330, Volume 330, p. 245
- Reid, M.J., Schneps, M.H., Moran, J.M., et al. 1988, *ApJ*, 330, 809
- Sjouwerman, L.O., Capen, S.M., & Claussen, M.J., 2009, *ApJ*, 705, 1554
- Skrutskie, M.F., Cutri, R.M., Weinberg, R., et al., 2006, *AJ*, 131, 1163
- Trapp, A.C., Rich, R.M., Morris, M.R., Sjouwerman, et al. 2018, *ApJ*, 861, 75
- Wright, E.L., Eisenhardt, P.R.M., Mainzer, A.K., et al., 2010, *AJ*, 140, 1868